Mouse model of human coronavirus (HCoV)-NL63: comparison with rhinovirus-(RV)-A1B and effects of prior RV infection

J. Kelley Bentley, Jordan E. Kreger, Haley A. Breckenridge, Shilpi Singh, Yiran Li and Marc B. Hershenson
Dept. of Pediatrics, University of Michigan Medical School, Ann Arbor, Michigan

University of Michigan Medical School

ABSTRACT

Introduction: HCoV-NL63 is one of seven coronaviruses which cause respiratory infections in humans. While HCoV-NL63 usually causes minor respiratory tract infections, it employs angiotensin-converting enzyme 2 (ACE2) as a receptor, similar to SARS-CoV2. We sought to establish a mouse model of HCoV-NL63, compare with an established model of RV-A1B, and determine the effect of prior RV-A1B infection on HCoV-NL63 replication. **Methods:** HCoV-NL63 (BEI Resources) was propagated in LLC-MK2 cells stably expressing human ACE2 (hACE2). RV-A1B (ATCC) was grown in HeLa-H1 cells and partially purified by ultracentrifugation. Adult (6-8 week) C57BL6/J or B6.Cg-Tg(K18-ACE2)2Prlmn/J mice expressing hACE2 protein in the airway epithelium (K18-ACE2 mice) were infected intranasally with sham cell lysate or HCoV-NL63 (1 x 10^5 $TCID_{50}$ units). Additional C57BL/6 mice were infected with 1 x 10^6 PFU RV-A1B in 50 mL PBS. Lungs were assessed for vRNA, bronchoalveolar lavage (BAL) cells, histology, HCoV-NL63 non-structural protein (nsp)-3 expression and gene expression by next generation sequencing and qPCR. Finally, selected mice were infected with RV-A1B four days before HCoV-NL63. **Results**: Compared to lungs from wild-type mice, hACE2 mice infected with HCoV-NL63 for two days showed higher levels of vRNA (78±13 vs. 0 copies/mg RNA), BAL neutrophils (49±8 vs 3.8±0.8 x 10^4/mL), BAL lymphocytes (19±2 vs 3.2±0.2 x 10^4/mL), peribronchial and perivascular infiltrates, and expression of nsp-3, evidence of a replicative infection. Next generation sequencing of lungs from HCoV-NL63-infected mice showed >1.5 fold increases in IFN-α2, IFN-β1, IFN-λ3 and several IFN-stimulated genes. In contrast, lungs from RV-A1B-infected mice showed >1.5 fold expression of IFN-γ, IL-1β, NLRP3, TLR2, as well as C-C and C-X-C chemokines. qPCR results confirmed higher mRNA expression of IFN-α2, IFN-β1, IFN-λ3 in lungs from HCoV-NL63-infected mice, and higher mRNA expression of IFN-γ, IL-1β, NLRP3, TLR2, CXCL2 and CXCL10 in lungs from RV-A1B infected mice. Both HCoV-NL63 and RV-A1B induced lung mRNA expression of IFN-stimulated genes. Finally, infection with RV-A1B four days before infection with HCoV-NL63 significantly decreased CoV-NL63 vRNA levels, BAL neutrophils and lymphocytes, peribronchial and perivascular infiltrates, and nsp3 expression. **Conclusion:** We have established a mouse model of HCoV-NL63 replicative infection, as evidenced by viral production of nsp3 and lung expression of IFNs and IFN-stimulated genes. Infection with RV-A1B induced a more pro-inflammatory phenotype than HCoV-NL63. Prior infection with RV-A1B reduced HCoV-NL63 replication and airway inflammation, consistent with IFN-dependent viral interference. Future work will examine the mechanisms underlying this viral interaction.

Supported by National Institutes of Health grants AI120526 and AI155444.

INTRODUCTION

We previously developed a mouse model of rhinovirus (RV)-A1B infection. However, mice infected with RV-A1B show limited viral replication. We sought to establish a mouse model of HCoV-NL63 by infecting transgenic mice expressing hACE2. We hypothesized that hACE2 in mice permits HCoV-NL63 infection. RV infection blocks SARS-CoV-2 replication in cultured airway epithelial cells (Dee et al. J Infect Dis 2021) and airway epithelial organoids (Cheemarla et al. J Exp Med 2021). We therefore also tested whether RV-A1B infection blocks HCoV-NL63 infection in our *in vivo* model.

METHODS

Antibodies to HCoV-NL63 proteins. Rabbit polyclonal antibodies against HCoV-NL63 nsp3 and nucleoprotein peptide sequences were generated (Genscript). Primary antibodies were labeled using AlexaFluor dye-conjugated N-hydroxy succinimidyl esters. ***Viral preparation***. HCoV-NL63 was grown in LLC-MK2 cells (both from BEI Resources). HCoV-NL63 infected LLC-MK2 cells were harvested by scraping, homogenization and centrifugation at 10,000 x *g*. Cell supernatants were used for infections. Viral cytopathic effects at 72 h post-infection was used to determine the tissue culture infectious dose ($TCID_{50}$). Primers from the HCoV-NL63 sequence (NC_005831.2) were used to measure viral copy number (vRNA) by qPCR, using a plasmid containing bases 1-540 as a copy number standard (GenScript). RV-A1B virus (ATCC) was grown in HeLa-H1 cells, concentrated by ultrafiltration with a 100 kD filter, and plaque assayed. ***Infection of mice***. K18-ACE2 mice (Jackson Labs) were genotyped using the vendor-recommended protocol and confirmed by hACE2 mRNA expression by qPCR. Eight-to-ten-week-old ACE2 or C57BL6/J mice were inoculated with 50 µL of 1 x 10^5 $TCID_{50}$ HCoV-NL63 intranasally and euthanized 1-7 days post-treatment. The 10,000 x *g* supernatant fluid from LLC-MK2 cells was used for sham infections. Selected K18-hACE2 mice were infected intranasally with 50 mL RV-A1B (1 x 10^6 PFU). ***Histology, immunofluorescence and immunoblotting***. Perfused mouse lungs were paraffin sectioned and stained with H&E or immunofluorescence with anti-HCoV nucleoprotein, anti-nsp3 and/or anti-double-stranded (ds)RNA (clone rJ2, Sigma-Aldrich). Lung lysates were probed with anti-nsp3 and β-actin (Sigma-Aldrich) by immunoblotting. ***Bronchoalveolar lavage (BAL)***. BAL cytospins were stained with H&E and differential counts determined from 200 cells. ***Next generation RNA sequencing (RNASeq)***. RNA library generation and next generation sequencing was performed by the University of Michigan Advanced Genomic Core. Total RNA was prepared using Trizol (InVitrogen), double purified using RNEasy spin columns (Qiagen) and enriched for mRNA using a Poly(A) mRNA Magnetic Isolation Module (New England Biolabs). cDNA libraries were prepared with a xGen Broad-range RNA Library Prep and Normalase UDI Primers (IDT). Samples were subjected to 151 bp paired-end sequencing using a NovaSeq S4 flow cell (Illumina). Reads were mapped to the reference genome GRCm38 (ENSEMBL 102) using STAR v2/7.8a and assigned count estimates to genes with RSEM v1/3.3. For RNASeq analysis, gene expression was estimated according to the expected count totals extracted through sequence alignment. Differential gene expression for HCoV-NL63 vs sham and RVA-1B vs sham was determined using R package DESeq2 v1/38.1. Wald test p values were adjusted for multiple testing using the procedure of Benjamini and Hochberg. Genes with an adjusted p value <0.05 were considered significant. Because of the small number of samples, we also defined differentially-expressed genes as those with a fold change of ≥ 1.5 or ≤ 0.66 and categorized them into biological process gene ontology groups using the R package clusterProfiler v4/6.0. We focused on 27 gene ontology groups related to the immune process. Genes encoding interferons (IFNs), IFN-stimulated genes (ISGs) and pro-inflammatory cytokines were selected for fold change comparisons. *Quantitative polymerase chain reaction (qPCR)*. First strand cDNA was prepared using the SuperScript IV system (Applied Biosystems). Transcript abundance relative to GAPDH was estimated by qPCR. ***Enzyme-linked immunosorbent assay (ELISA)***. BAL cytokines were measured by ELISA. We measured levels of IL-36α (MyBioSource), IL-1β (Invitrogen), IFN-α1 (Biolegend) and IFN-l2/3 (R&D Systems).

METHODS AND RESULTS

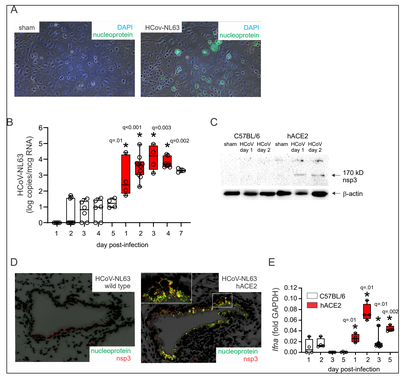

Figure 1. HCoV-NL63 produces a replicative in infection in K18-ACE2 mice. LLC-MK2 cells infected with sham cell supernatants (left) or HCoV-NL63 (right). Infection confirmed by staining with anti-HCoV-NL63 nucleoprotein. B. K18-hACE2 or C57BL6/J mice inoculated with 50 µL of HCoV-NL63 intranasally and harvested 1-7 days later. Mouse lung viral copy number measured by qPCR (total of 4 experiments, n = 2-10, undetectable vRNA designated as 1 copy/µg RNA; *different from wild-type mice, Kruskal-Wallis test). C. Sham- and HCoV-NL63-infected wild-type and K18-hACE2 lungs immunoblotted for nsp3 and β-actin. D. Sections stained for HCoV-NL63 nucleoprotein (green) and nsp3 (red). E. Lung IFN-α mRNA measured by qPCR (total of 2 experiments, n = 4-8, *different from wild-type mice, Kruskal-Wallis test). Box and whiskers plots show median, 25th and 75th percentiles (hinges of the box), and min and max values (whiskers).

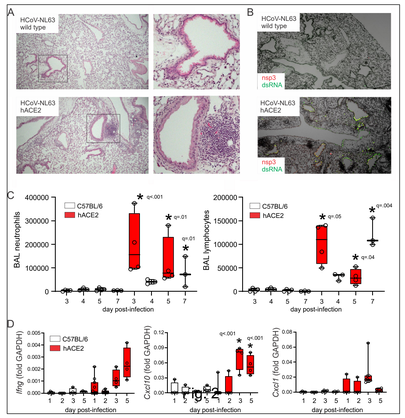

Figure 2. HCoV-NL63 induces lung inflammation in K18-ACE2 mice. K18-hACE2 or C57BL6/J mice inoculated with HCoV-NL63. A. Lung sections from wild-type (upper panel) and K18-hACE2 mice (lower panel) were stained with hematoxylin and eosin (H&E). B. Lung sections from wild-type (upper panel) and K18-hACE2 mice (lower panel) were immunostained for nsp3 (red) and dsRNA (green). C. BAL neutrophils (left panel) and lymphocytes (right panel) were significantly increased in hACE2 mice compared to wild-type mice (results from 2 separate experiments, n = 3-4, *different from wild-type mice, Kruskal-Wallis test. D. Lung mRNA expression was measured by qPCR (total of 2 experiments, n = 4-8, *different from wild-type mice, Kruskal-Wallis test).

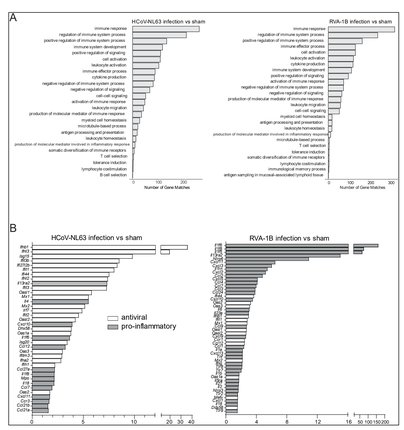

Figure 3. Next generation RNA sequencing. Following HCoV-NL63 infection, 133 genes were differentially expressed, with 51 significantly upregulated and 78 significantly downregulated). Of note, two ISGs, Isg20 and Ifi35 were increased. Following RV-A1B infection, 26 genes were differentially expressed, with 22 significantly upregulated and 4 significantly downregulated). The asthma-related genes gasdermin A (Gsdma), arachidonate 15-lipoxygenase (Alox15), GATA binding protein (Gata3) and interleukin 1 receptor antagonist (Il1rn), were increased. Aconitate decarboxylase 1 (Acod1) was also significantly upregulated.

A. Gene ontology analysis of transcripts induced by HCoV-NL63 (left panel) and RV-A1B infection (right panel) compared to sham infection. Immune response categories are shown. B. IFN, ISG and pro-inflammatory gene expression induced by HCoV-NL63 (left panel) and RV-A1B infection (right panel). Data represent mean fold increase vs. sham infection.

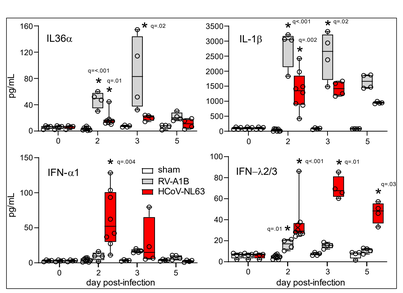

Figure 4. BAL cytokines in HCoV-NL63- and RV-A1B-infected mice. We measured the time course of selected cytokines in the BAL by ELISA. IL-36α and IL-1β tended to be higher after RV-A1B infection, and IFN-α1 and IFN-λ2/3 tended to be higher after HCoV-NL63 infection (two experiments, n = 4-8, *different from same day sham, Kruskal-Wallis test).

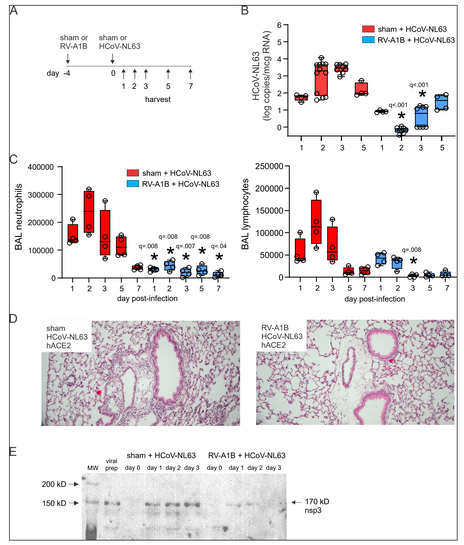

Figure 5. RV-A1B pre-infection attenuates HCoV-NL63 replication and airway inflammation in K18-ACE2 mice. A. Mice were infected with sham or RV-A1B four days before sham or HCoV-NL63 infection. B. Lung RNA was harvested two days after HCoV-NL63 infection for viral copy number analysis by qPCR (total of 3 experiments, n = 4-12, samples with undetectable vRNA were designated as 1 copy/µg RNA to allow graphing; *different from sham-infected mice, Kruskal-Wallis test). C. BAL cytospins stained with H&E and differential counts from 200 cells. BAL neutrophils (left panel) and lymphocytes (right panel) are shown (results from 2 separate experiments, n = 4 per group, *different from sham-infected mice, Kruskal-Wallis test. D. Lung sections from mice infected with sham and HCoV-NL63 (left panel) or with RV-A1B and HCoV-NL63 (right panel) were stained with H&E. E. Lung lysates from sham- and HCoV-NL63-infected hACE2 mice (left) and RV-A1B and HCoV-NL63-infected hACE2 mice (right) were immunoblotted for nsp3. Box and whiskers plots show median, 25th and 75th percentiles, and min and max values.

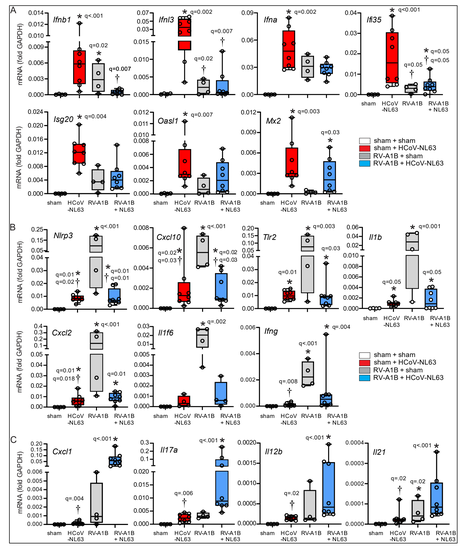

Figure 6. Effect of prior RV-A1B infection on HCoV-NL63-induced mRNA expression. A. Lung mRNA expression of selected genes encoding IFNs and ISGs (panel A) was measured by qPCR (total of 2 experiments, n = 4-8, *different from sham infection, †different from sham + HCoV-NL63, Kruskal-Wallis test). B. Lung mRNA expression of selected pro-inflammatory genes was measured by qPCR (total of 2 experiments, n = 4-8, *different from sham infection, †different from RV-A1B + sham infection, Kruskal-Wallis test). C. mRNAs showing an additive for synergistic effect of RV-A1B and HCoV-NL63 (total of 2 experiments, n = 4-8, *different from sham infection, †different from RV-A1B + HCoV-NL63 infection, Kruskal-Wallis test). Box and whiskers plots show median, 25th and 75th percentiles, and min and max values.

SUMMARY AND CONCLUSIONS

- We established a mouse model of HCoV-NL63 using mice expressing human ACE2 under control of the keratin 18 promoter. Compared to wild-type mice, hACE2 mice showed significantly higher levels of HCoV-NL63 vRNA and nsp3, a non-structural viral protein that is produced in replicating virus. In addition, HCoV-NL63-infected hACE2 mice showed increased BAL neutrophils and lymphocytes, as well as peribronchial and perivascular infiltrates compared to mock-infected controls. Together these data suggest that HCoV-NL63 causes a replicative infection in hACE2 transgenic mice. Our work provides a BSL-2 animal model to study human CoV infection in mice.
- We also found that prior RV-A1B infection significantly reduced HCoV-NL63 replication and viral-induced peribronchial inflammation, an example of viral interference. However, in our model, we did not find evidence that RV-A1B interferes with HCoV-NL63 infection by enhancing IFN production.
- Finally, we found that mRNA expression of many pro-inflammatory genes was significantly higher after RV-A1B infection than HCoV-NL63 infection, including Tlr2, Il1b, Nlrp3, Nlrc3, Ifng, Cxcl2, and Cxcl10. BAL protein levels of IL-36α and IL-1β also tended to be higher in RV-A1B-infected mice. On the other hand, HCoV-NL63-infected mice showed increased expression of IFNs including Ifna, Ifnb1, Ifnla, and ISGs including Ifi35, Isg20, Oasl1 and Mx2. We found similar results for BAL protein levels of IFN-α1 and IFN-λ2/3. Together these data suggest that HCoV-NL63 infection promotes less airway inflammation than RV-A1B infection.
- This model may provide insight into the mechanisms underlying HCoV-induced asthma exacerbations and viral interference.